Experimental studies of micromegas detectors with different micro-meshes*

YANG He-Run(杨贺润) HU Bi-Tao(胡碧涛)[1)] ZHANG Xiao-Dong(张小东) ZOU Chun-Yan(邹春燕)

School of Nuclear Science and Technology, Lanzhou University, Lanzhou 730000, China

Abstract: The structure of micromegas (micro-mesh gaseous structure) detectors with different micro-meshes of stainless steel wire woven netting and Ni foil has been presented. The counting rates, energy resolution, gain, discharge probability and time resolution have been measured. Wider counter plateaus and gain for the developed detector were obtained. Excellent energy resolution of the micromegas detector, 17% (FWHM) based on Ni foil micro-mesh and 25% (FWHM) based on stainless steel wire woven netting micro-mesh, has been obtained for the 5.9 keV photon peak of the ^{55}Fe X-ray source in an Ar/CO_2(10%) gas mixture. The best time resolution at −620 V micro-mesh voltage and −870 V drift voltage is 14.8 ns for cosmic rays in an Ar/CO_2 (10%) gas mixture. These results satisfy the basic demand of the micromegas detector preliminary design.

Key words: micromegas, counter plateaus, energy resolution, discharge probability, time resolution

PACS: 29.40.Gx, 29.40.Cs, 28.20.-v **DOI:** 10.1088/1674-1137/35/2/013

1 Introduction

As a kind of MPGD (micro pattern gaseous detectors) [1], the micromegas (micro-mesh gaseous structure) detector was developed by Y. Giomataris and G. Charpak in Saclay, France [2]. The micromegas detector, which is a gaseous detector based on the amplification of electron avalanches in short gaps of the order of 100 μm at atmospheric pressure, is a very asymmetric two-parallel plate avalanche chamber. Thanks to the small gap and high field, the positive ions released in the avalanche gap can be collected very quickly. This induces very fast signals with very small ion tail. Because of its advantages of high space and time resolution, insensitivity to discharges, simplicity of construction and capacity for identifying and reducing some sources of background, it is widely used in nuclear physics experiments [3]. The aim of this work is to perform a systematic study of the properties of the micromegas detector based on different micro-meshes.

2 Experimental setup

In our experiment, the tests were performed with different micro-meshes. The structure of the micromegas detector prototype is shown in Fig. 1. The conversion space is 3 mm and the 160 μm amplification gap is defined by stretching nylon fishing lines with a diameter of (160±5) μm every 2 mm on the anode plane made of a printed circuit board (PCB), perpendicular to the strips. The drift cathode is made of a stainless steel wire woven netting (500LPI) and the diameter of each line is 24 μm. The micro-mesh in one detector is made of a Ni foil (600LPI) with thickness of 5 μm, while in the other detector it is stainless steel wire woven netting of 18 μm stainless steel wire with 600LPI.

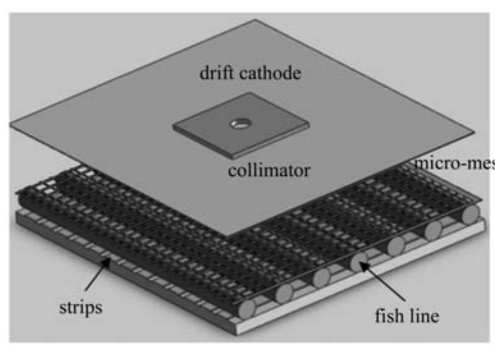

Fig. 1. Schematic view of the micromegas detector.

Received 24 May 2010

* Supported by National Natural Science Foundation of China (10575046,10775062) and Program for New Century Excellent Talents in University

1) E-mail: hubt@lzu.edu.cn

The micromegas detector was operated in different Ar/CO_2 mixtures at a normal pressure and temperature. Measurements were carried out using a ^{55}Fe source X-source which was positioned in such a way that a collimated beam (ϕ1 hole) of X-rays perpendicularly entered the conversion gap (Fig. 1). Time tests were performed with cosmic rays. Negative potentials were applied to both the drift electrode and the micro-mesh electrode. The signals of the detector were induced on the micro-mesh and anode electrode (PCB readout strips) with different types of preamplifiers. The charge sensitive preamplifier Ortec 142PC was used for energy signals and the preamplifier Ortec 142 A fast-timing output for time signal.

3 Results and discussions

Figure 2 shows a pulse height spectrum obtained with a ^{55}Fe source in the Ar/CO_2 (10%) gas mixture. Fig. 2(a) indicates the energy resolution (FWHM) of the micromegas detector based on the Ni foil micro-mesh is about 17%. The energy resolution is better than the one in Cussonneau's work [4], where the energy resolution was 25% with a Ar/CO_2(26%) mixture and a 100 μm amplification gap. Fig. 2(b) tells us that the energy resolution (FWHM) of the detector based on stainless steel wire woven netting micro-mesh is about 25% which is better than the results got in the USTC work [5], where the energy resolution (FWHM) was 27% with Ar/iC_4H_{10}(10%) gas mixture and 100 μm amplification gap. Before we go further, one thing we have to mention here is that in Refs. [4, 5] the Ni foil and stainless steel wire woven netting used in the detector was stretched by mechanical force rather than thermal expansion and contraction used in the present work. Therefore, we may safely draw a conclusion that pasting the micro-mesh with thermal expansion and contraction can provide better results. Further, comparing the results shown in Fig. 2(a) and Fig. 2(b), the micro-mesh property is a very important factor in energy resolution.

In order to know the suitable working conditions of the detector, its counter plateau was measured and the results are shown on Fig. 3. The length and slope of the counter plateaus are about 150 V and 6%/100 V. With the help of Fig. 3, we can choose the optimal working conditions. The length of the counter plateaus is longer than that of Ref. [6].

The measured gain and discharge rate as a function of micro-mesh voltage can be found in Fig. 4. Fig. 4(a) is the gain and discharge rate for the micromegas detector based on Ni foil micro-mesh in an Ar/CO_2(10%) gas mixture, whereas Fig. 4(b) is that based on stainless steel wire woven netting micro-mesh in an Ar/CO_2(15%) gas mixture. With a reasonable field in the avalanche gap, gains greater than 10^4 are achievable. In addition, its gain can be large enough so that it doesn't need an additional preamplifier [6, 7]. We stopped testing the energy spectrum when the detector read-out signal amplitude exceeded the preamplifier limit. The discharge probability per particle was found to increase fairly linearly with the gas gain for 5 mCi ^{55}Fe, as shown in Fig. 4. The discharge is worse than the one in the PSI (Paul Scherrer Institute)'s work [8], where the discharge rate was 10^{-6} for 10^3–10^4 gain with Ar/CO_2 (7% or 40%) gas mixture for the two kinds of beams, namely 215 MeV/c π^+ and 350 MeV/c protons.

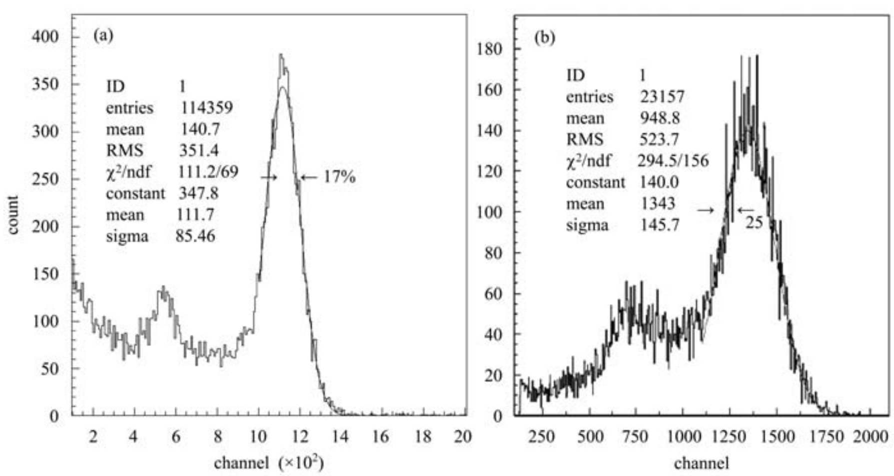

Fig. 2. ^{55}Fe X-ray energy spectrum in an Ar/CO_2(10%) gas mixture at the micro-mesh voltage of −590 V and drift voltage of −630 V. (a) Energy resolution of the micromegas detector based on Ni foil micro-mesh is 17% (FWHM); (b) Energy resolution of the micromegas detector based on stainless steel wire woven netting micro-mesh is 25% (FWHM).

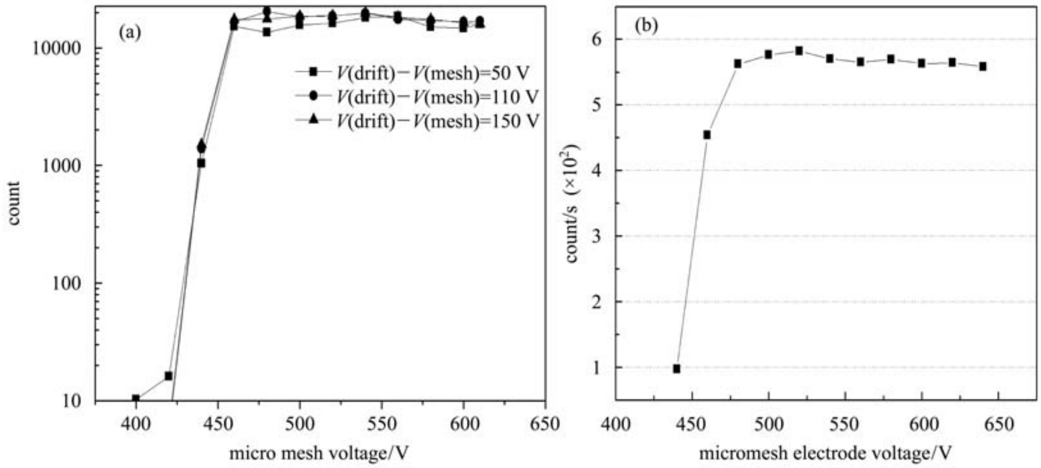

Fig. 3. Counter plateaus of the micromegas detector in an Ar/CO_2 (10%) gas mixture with a ^{55}Fe X ray source. (a) Counter plateaus of the micromegas detector based on Ni foil micro-mesh; (b) Counter plateaus of the micromegas detector based on stainless steel wire woven netting micro-mesh.

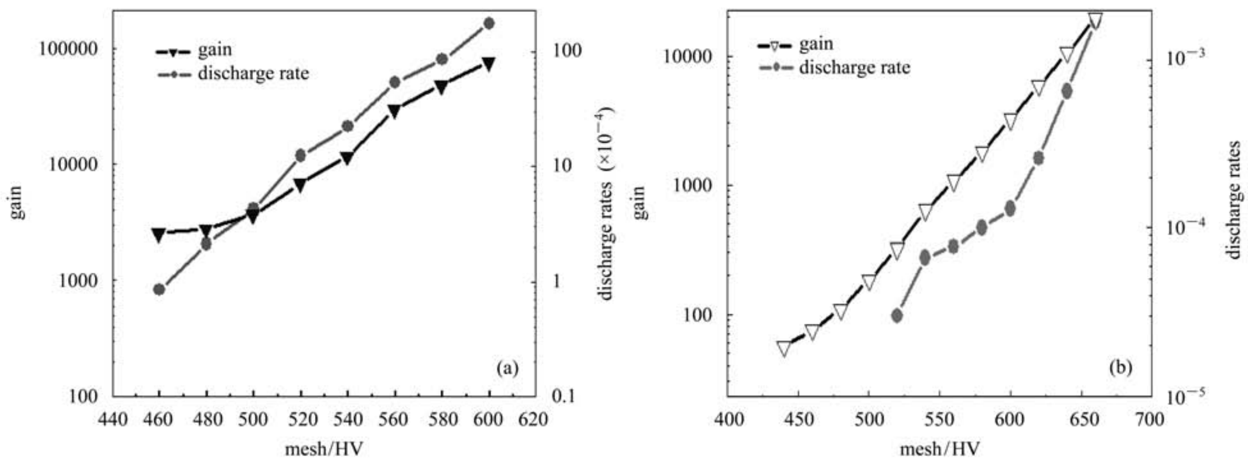

Fig. 4. Experimental gain and discharge rates of the micromegas detector as a function of the micro-mesh voltage for 5 mCi ^{55}Fe source. (a) The gains and discharge rates as a function of the micro-mesh voltage based on Ni foil in an Ar/CO_2 (10%) gas mixture; (b) The gains and discharge rates as a function of the micro-mesh voltage based on stainless steel wire woven netting in an Ar/CO_2 (15%) gas mixture.

The time resolution for individual events results from the fluctuation of the rise time of the signal. Both the fast-moving electrons and the slowly drifting ions contribute to the signal amplitude. Fig. 5 exhibits the time signal using the current-sensitive preamplifier Ortec VT120A with fast-timing output. The sharp peak at the beginning of the signal is induced by the avalanche electrons between the micromesh cathode and the PCB anode, and the long tail is due to the ions. Since the drifting velocity of electrons is much faster than that of the ions, a rising time of the signal less than 6 ns is obtained although the ion tail is about 35 ns. Because the signal rising time is less than 6 ns and the total duration does not exceed 100 ns, the micromegas detector is able to supply nice time resolution and high counting rate.

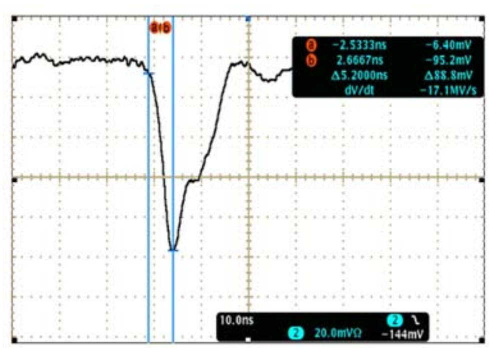

Fig. 5. Fast-timing output signal at a gain of 9300 using the Ortec VT120A. Electron signal and the ion tail are developed within 6 ns and 35 ns respectively.

The time resolution was measured in a fairly straightforward manner. We triggered the oscilloscope with the coincidence between the signals from the micromegas detector and a photomultiplier induced by cosmic rays, and measured the time between the micromegas detector signal and the photomultiplier signal. The time spectrum of the micromegas detector based on Ni foils micro-mesh is shown in Fig. 6. The time resolution σ is 14.8 ns for cosmic rays at −620 V micro-mesh voltage and −870 V drift voltage. The small amplification gap produces a narrow avalanche to achieve excellent time resolution.

Meanwhile, we tested the dependence of time resolution on the micro-mesh and drift voltage. Fig. 7(a) is the time resolution at the constant drift voltage and different micro-mesh voltages and Fig. 7(b) is that at different drift voltages and the constant micro-mesh voltage. According to Fig. 7, when the drift voltage is kept constant, the time resolution fluctuates around a certain value, whereas under the condition of constant micro-mesh voltage, the time resolution becomes better and better with the rising drift voltage. The time resolution is the temporal stability with which the signal begins. This is logical since the longitudinal diffusion is less important for a small amplification space. The drift speed of the electrons plays an important role in time resolution, the faster or the earlier the signal appears, the less the electrons have diffused [9]. The electron drift velocity depends on both the electric field and the gas mixture characteristics. The simulated results of the drift velocity as a function of the electric field in Ar/CO_2(10%) gas mixtures is illustrated in Fig. 8. The time resolution becomes better with the increase of the drift voltage, which is caused by the raised drift speed with the increasing electric field.

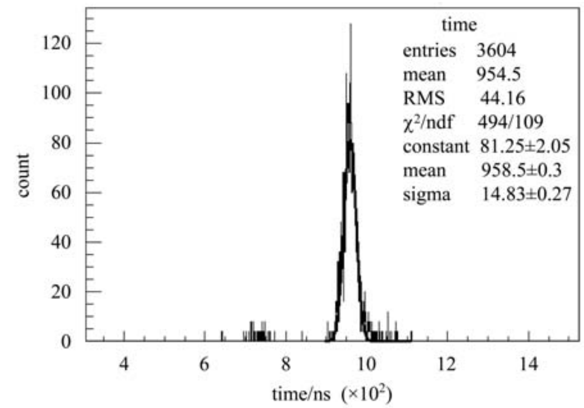

Fig. 6. The time resolution spectrum of the micromegas detector based on Ni foils micro-mesh.

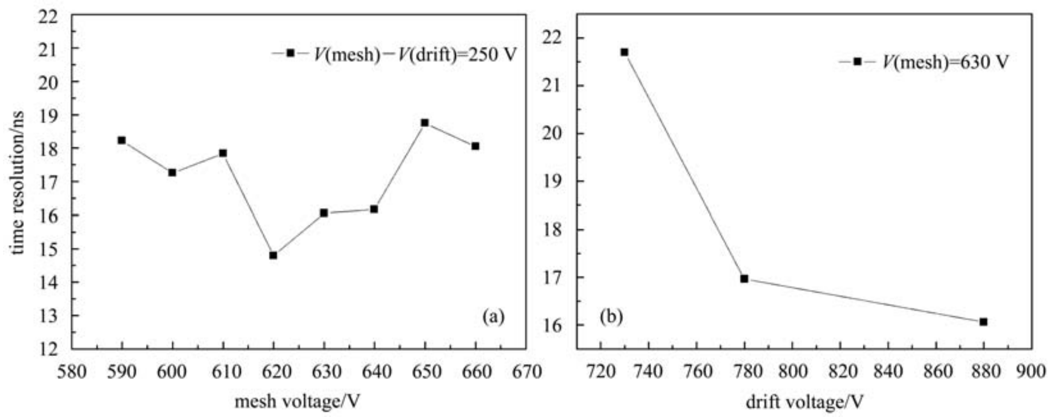

Fig. 7. The time resolution as a function of the voltage for cosmic rays. (a) The time resolution as a function of the micro-mesh voltage. (b) The time resolution as a function of the drift voltage.

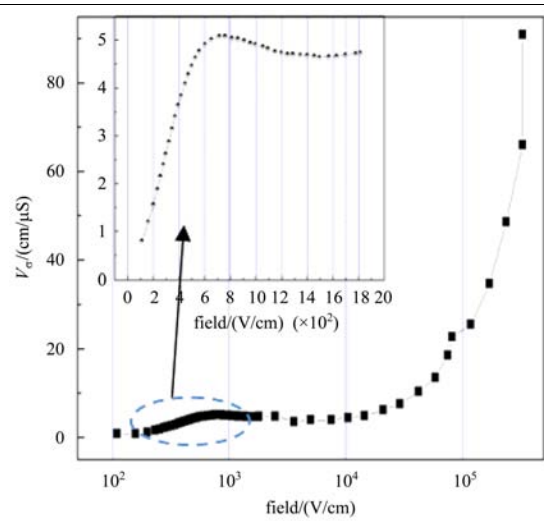

Fig. 8. The simulated drift velocity of electrons as a function of the electric field by simulation program GARFIELD [10] and Magboltz [11]. The gas mixture characteristics: Ar/CO_2 (10%), $T = 300$ K, and 1atm.

4 Conclusion

In this paper, the measured results of the micromegas detector developed are presented. The results indicate that the micromegas detector with Ni foil micro-mesh or stainless steel wire woven netting micro-mesh can reach rather good operational states. However, using ^{55}Fe radioactive 5.9 keV X-rays source in an Ar/CO_2 (10%) gas mixture, the energy resolution of the detector with the Ni foil micro-mesh can reach up to 17 % (FWHM), which is much better than the one with stainless steel wire woven netting micro-mesh whose energy resolution is 25% (FWHM). Large counter plateaus and gain for the developed detector were obtained. The dependence of time resolution on the micro-mesh and drift voltage was carefully studied. The best time resolution is 14.8 ns at −620 V micro-mesh voltage and −870 V drift voltage. All the measured results obtained by us indicate that the performances of the detector, such as energy resolution, gas gain and the time, depend on many parameters, which need to be optimized for a particular purpose.

References

1 Cussonneau J P, Labalme M, Lautridou P et al. Nucl. Instrum. Methods A, 1998, **419**: 452
2 Giomataris Y, Rebourgeard Ph, Robert J P et al. Nucl. Instrum. Methods A, 1996, **376**: 29
3 Charpak G, Derré J, Giomataris Y et al. Nucl. Instrum. Methods A, 2002, **478**: 26
4 Cussonneau J P, Labalme M, Lautridou P et al. Nucl. Instrum. Methods A, 1998, **31**: 452
5 GUO Jun-Jun, WANG Xiao-Lian, TANG Hao-Hui et al. Chin. Phys. C, 2010, **34**: 482
6 Derré J, Giomataris I. Nucl. Instrum. Methods A, 2001, **461**: 74
7 Delbart A, Derré J, Giomataris Y et al. Nucl. Instrum. Methods A, 2002, **478**: 205
8 Perroud J P, Ronga F. http://cdsweb.cern.ch/record/684720/files/lhcb-99-020.pdf
9 Pancin J, Chaminade T, Drouart A et al. Journal of Instrumentation, 2009, **12**: 12
10 Veenhof R. Garfield drift chamber simulation program. http://garfield.web.cern.ch/gar_eld/and the links therein
11 Biagi S. Magboltz program to compute gas transport parameters, Version 2.2, CERN. http://www.jlab.org/~grimm/Qweak/Garfield/html/garfield_33.html and the links therein